

GoAgent: Group-of-Agents Communication Topology Generation for LLM-based Multi-Agent Systems

Hongjiang Chen¹, Xin Zheng², Yixin Liu³, Pengfei Jiao¹, Shiyuan Li³, Huan Liu¹,
Zhidong Zhao¹, Ziqi Xu², Ibrahim Khalil², Shirui Pan³,

¹School of Cyberspace, Hangzhou Dianzi University, Hangzhou, China,

²School of Computing Technologies, RMIT University, Melbourne, Australia,

³School of Information and Communication Technology, Griffith University, Goldcoast, Australia
{hchen, pjiao, huanliu, zhaozd}@hdu.edu.cn, {xin.zheng2, ziqi.xu, ibrahim.khalil}@rmit.edu.au,
{yixin.liu, shiyuan.li, s.pan}@griffith.edu.au

Abstract

Large language model (LLM)-based multi-agent systems (MAS) have demonstrated exceptional capabilities in solving complex tasks, yet their effectiveness depends heavily on the underlying communication topology that coordinates agent interactions. Within these systems, successful problem-solving often necessitates task-specific group structures to divide and conquer subtasks. However, most existing approaches generate communication topologies in a node-centric manner, leaving group structures to emerge implicitly from local connectivity decisions rather than modeling them explicitly, often leading to suboptimal coordination and unnecessary communication overhead. To address this limitation, we propose **GoAgent** (Group-of-Agents), a communication topology generation method that explicitly treats *collaborative groups* as the atomic units of MAS construction. Specifically, GoAgent first enumerates task-relevant candidate groups through an LLM and then autoregressively selects and connects these groups as atomic units to construct the final communication graph, jointly capturing intra-group cohesion and inter-group coordination. To mitigate communication redundancy and noise propagation inherent in expanding topologies, we further introduce a conditional information bottleneck (CIB) objective that compresses inter-group communication, preserving task-relevant signals while filtering out redundant historical noise. Extensive experiments on six benchmarks demonstrate the state-of-the-art performance of GoAgent with 93.84% average accuracy while reducing token consumption by about 17%.

1 Introduction

Large language model (LLM)-based multi-agent systems (MAS) have become a promising approach for solving complex tasks (Tran et al., 2025), ranging from code generation (Zhang et al., 2024a) to mathematical reasoning (Yao et al., 2023) and

multi-step decision-making (Guo et al., 2026). The core of any MAS is its communication topology, a directed graph that governs how agents interact, share information, and coordinate their efforts (Wu et al., 2024; Liang et al., 2024; Wang et al., 2025a). Recent studies show that the underlying organizational structure impacts the overall performance of MAS more than the capabilities of individual agents (Qian et al., 2025; Rizvi-Martel et al., 2026; Zhou et al., 2026a). Consequently, designing communication topologies that ensure both effective problem-solving and efficient token usage has become a central challenge.

Early approaches to topology design relied on static, manually crafted structures, such as chains for sequential reasoning (Zhang et al., 2024b), trees for hierarchical deliberation (Zhou et al., 2024), and fully connected graphs for exhaustive debate (Hu et al., 2024). While effective in narrow domains, these fixed topologies lack the flexibility to adapt to diverse task requirements (Liu et al., 2025). To overcome this rigidity, subsequent research introduced deep learning techniques to automatically learn topologies based on predefined templates. Methods like AgentPrune (Zhang et al., 2025a), AgentDropout (Wang et al., 2025b), G-Designer (Zhang et al., 2025b), and GTD (Jiang et al., 2025) take a dense template graph and optimize it by pruning or reweighting edges for specific tasks. However, these template-based methods remain bounded by the initial agent sets and connectivity patterns. Most recently, ARG-Designer (Li et al., 2025) moved beyond these template constraints by proposing an autoregressive approach that dynamically generates the collaboration graph from scratch, sequentially adding agents, assigning roles, and establishing connections.

Despite these advancements, existing topology generation methods share a fundamental flaw: they operate under a node-centric construction paradigm. As illustrated in Figure 1(a), each agent

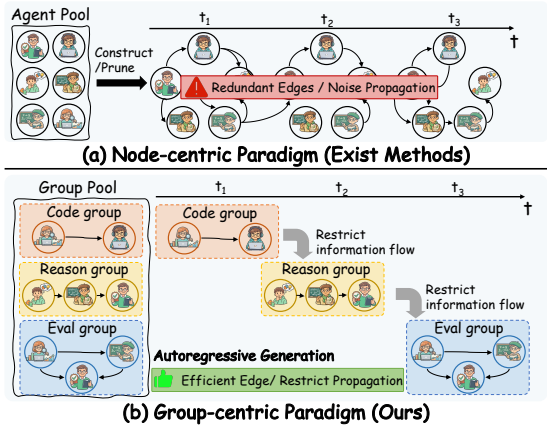


Figure 1: The comparison of two paradigms: (a) node-centric and (b) group-centric graph generation.

is treated as an individual node and the topology is built by predicting agents and their connections step-by-step, resulting in isolated local decisions without a macroscopic view of the overall collaborative workflow. This localized generation process introduces two critical limitations (Barkoczi and Galesic, 2016). *First*, it hinders effective inter-agent coordination. Complex reasoning tasks naturally require a divide and conquer strategy executed by tightly coupled groups (Betti et al., 2025), such as a cohesive sub-team for problem solving consisting of a decomposer, a solver, and a verifier. Under the node-centric paradigm, these essential higher-order structures are not explicitly modeled; instead, they are expected to emerge implicitly from ad-hoc edge predictions, frequently resulting in disjointed workflows and suboptimal problem-solving (Pescetelli et al., 2021). *Second*, it exacerbates communication inefficiency and noise propagation (Shen et al., 2025; Zhou et al., 2026b). Without explicit group boundaries to structure information exchange, the generated graphs tend to form dense, unconstrained connections. This uncontrolled connectivity not only incurs substantial token overhead due to redundant message passing, but also allows task-irrelevant historical noise to accumulate and distract agents from critical signals. These limitations raise a critical question:

Can we move beyond the node-centric paradigm and design communication topologies using higher-level abstractions that explicitly capture and utilize collaborative group structures?

We answer this question by proposing **GoAgent** (Group-of-Agents), a communication topology generation method that fundamentally shifts

the paradigm by explicitly treating collaborative groups as the atomic units for construction (Figure 1(b)). Given a specific task query, GoAgent first prompts an LLM to enumerate a set of task-relevant candidate groups, where each group encapsulates a coherent cluster of expert roles tailored for a specific subtask. A learned autoregressive graph generation model then systematically selects and connects these predefined groups to construct the final communication topology. This group-level generation inherently preserves strong intra-group cohesion while explicitly directing inter-group coordination. To address the issue of communication inefficiency and noise propagation inherent in expanding topologies, GoAgent incorporates a Conditional Information Bottleneck (CIB) mechanism into the graph generation process. Taking the specific task as the condition, the CIB layer actively compresses inter-group communication features, thereby retaining only the strictly necessary task-relevant signals and filtering out redundant historical noise. Our main contributions are summarized as follows:

- **New Paradigm.** We identify the inability of node-centric methods to explicitly model collaborative structures, proposing a group-centric paradigm that treats agent groups as atomic units of construction.
- **Novel Method.** We develop GoAgent, an autoregressive model bridging LLM-derived agent groups with graph generation, and introduce CIB to adaptively compress redundant communications.
- **Experimental Validation.** Experiments on six benchmarks show that GoAgent achieves state-of-the-art accuracy while reducing token consumption, establishing a new standard for efficient multi-agent system design.

2 Preliminaries

2.1 Problem Formulation

We study the problem of automatically constructing communication topologies for LLM-based MAS. Given a task query Q , the objective is to generate a communication structure that coordinates a set of agents to collaboratively solve the task.

Agents. Let $\mathcal{V} = \{v_1, \dots, v_N\}$ denote a set of N candidate agents. We instantiate each agent $v_i \in \mathcal{V}$ by assigning a role-specific system prompt (e.g.,

“Math Solver” or “Code Reviewer”) to a shared large language model to define its expertise. Given an input prompt \mathcal{P}_i , agent v_i generates a natural language response $\mathcal{R}_i = v_i(\mathcal{P}_i)$. Agents communicate via prompt composition: if the topology contains a directed edge from v_i to v_j , the response \mathcal{R}_i is appended to the input prompt of v_j as context, facilitating information flow across the system.

Collaborative Groups. To capture structured cooperation among agents, we introduce collaborative groups as higher-order coordination units. Each group represents a structured collaboration pattern among a subset of agents and is defined as $M_i = (\mathcal{S}_i, \mathcal{E}(\mathcal{S}_i))$, where $\mathcal{S}_i \subseteq \mathcal{V}$ denotes the subset of agents participating in group M_i , and $\mathcal{E}(\mathcal{S}_i)$ denotes the predefined communication relations (e.g., fully connected or chain) among agents within the group. Let $\mathcal{M} = \{M_1, \dots, M_K\}$ denote the set of collaborative groups.

Group-Level Communication Graph. Based on these collaborative groups, we construct a group-level communication graph

$$\mathcal{G} = (\mathcal{M}, \mathcal{E}), \quad (1)$$

where \mathcal{E} represents communication dependencies between groups. Each edge $e_{ij} \in \mathcal{E}$ indicates that information produced by group M_i can be transmitted to group M_j . The final communication topology among agents is induced jointly by the intra-group relations $\mathcal{E}(\mathcal{S}_i)$ and the inter-group dependencies \mathcal{E} .

Topology Generation. Given a task query \mathcal{Q} , the goal is to generate the group-level communication graph \mathcal{G} . Groups are generated sequentially, and each newly generated group may establish connections with previously constructed groups. Formally, the generation distribution is defined as

$$P(\mathcal{G}|\mathcal{Q}) = \prod_{i=1}^{|\mathcal{M}|} P(M_i|\mathcal{G}_{<i}, \mathcal{Q}) \prod_{j<i} P(e_{ji}|M_i, \mathcal{G}_{<i}, \mathcal{Q}), \quad (2)$$

where $\mathcal{G}_{<i}$ denotes the partial graph consisting of the first $i - 1$ generated groups. The first term models collaborative group selection, while the second term predicts communication edges between the newly generated group and previously constructed groups.

2.2 Information Bottleneck

The information bottleneck (IB) principle (Tishby et al., 2000) seeks a compressed representation \tilde{X}

of signals X that preserves the maximum information relevant to a target variable Y . The standard IB objective is formulated as minimizing:

$$\mathcal{L}_{\text{IB}} = -I(\tilde{X}; Y) + \beta I(\tilde{X}; X), \quad (3)$$

where β serves as a Lagrange multiplier that balances the trade-off between accurately predicting Y and effectively compressing X .

While standard IB compresses information unconditionally, it can be extended to the CIB (Gondek and Hofmann, 2003) by introducing a condition variable Z . CIB seeks to extract \tilde{X} that is maximally informative about Y while compressing X , all conditioned on Z :

$$\min \mathcal{L}_{\text{CIB}} = -I(\tilde{X}; Y|Z) + \beta I(\tilde{X}; X|Z). \quad (4)$$

By conditioning on Z , CIB ensures that the compression selectively filters out noise while preserving the specific structural or semantic patterns dictated by the condition Z .

3 Methodology

The primary goal of GoAgent is to generate a task-specific, group-level communication topology for MAS. Unlike existing node-centric approaches that predict individual agents step-by-step, we introduce a group-centric paradigm where high-level collaborative groups serve as the generative atomic units. This macroscopic approach significantly reduces the search space and aligns better with human-like organizational structures.

As formulated in Eq. (2), GoAgent factorizes the generation of topology \mathcal{G} into an autoregressive sequence of group selections and edge predictions. The pipeline consists of four phases: (1) encoding the task query and discovering candidate groups; (2) autoregressively generating groups and their communication edges; (3) applying a CIB layer to compress historical communication signals; and (4) supervised training on curated ground-truth trajectories. The pseudo-code is provided in Appendix B.

3.1 Task Encoding and Group Discovery

We first map unstructured text, including both the task requirements and the agent descriptions, into a continuous vector space.

Task Encoding. Given a task query \mathcal{Q} , we encode it into a global task representation $\mathbf{z}_{\mathcal{Q}} \in \mathbb{R}^d$ using a pre-trained sentence encoder followed by a feed-forward network (FFN):

$$\mathbf{z}_{\mathcal{Q}} = \text{FFN}(\text{SentenceEncoder}(\mathcal{Q})). \quad (5)$$

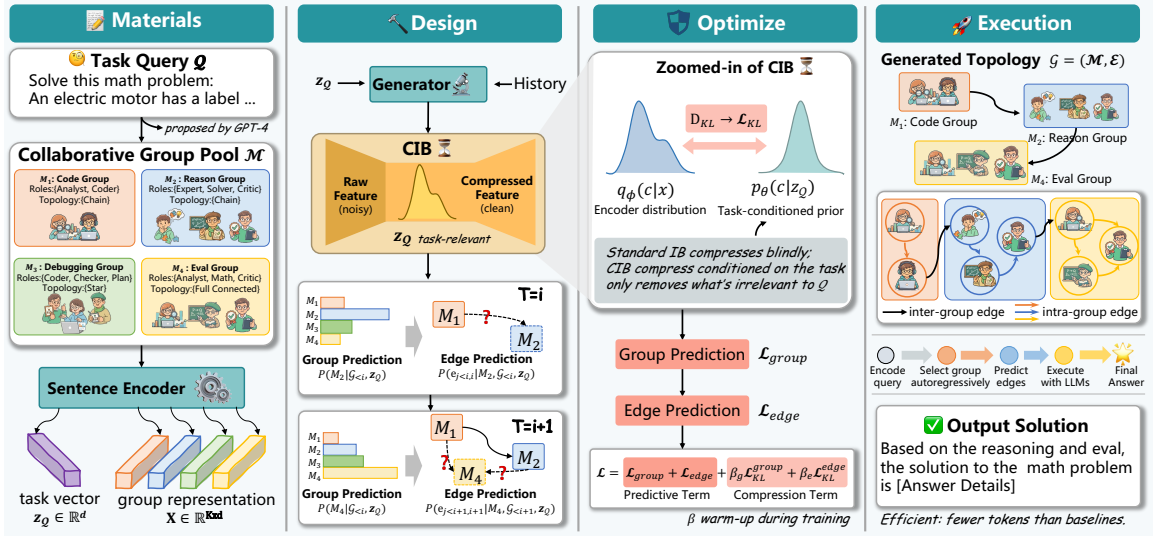


Figure 2: Overview of the proposed GoAgent.

This representation \mathbf{z}_Q serves as the global condition guiding all subsequent generation steps.

Collaborative Group Discovery. Instead of selecting individual agent instances, GoAgent samples from a predefined pool of K task-relevant collaborative groups. To construct this candidate space, we prompt a large language model (e.g., GPT-4) with domain-specific instructions to propose K expert groups (e.g., $K = 16$). Each group M_i is defined by a structured schema: (Name, Expertise, Roles, Intra-Topology). For example, a group might be defined as Name: “Code Debugging Group”, Expertise: “Identifies and fixes logical errors in code”, Roles: “[Code Reviewer, Syntax Checker, Logic Validator]”, and Intra-Topology: “Sequential Pipeline”. The intra-group edges $\mathcal{E}(S_i)$ are LLM-induced during this discovery phase and serve as fixed templates (e.g., fully connected for brainstorming, or sequential for refinement). These templates are rigidly enforced whenever the group is instantiated, allowing the autoregressive generator to focus entirely on the higher-level inter-group dependencies \mathcal{E} . We encode the textual descriptions of these K groups using the same sentence encoder to form a candidate embedding matrix $\mathbf{X} = [\mathbf{x}_1, \dots, \mathbf{x}_K] \in \mathbb{R}^{K \times d}$. To facilitate autoregressive generation, we augment \mathbf{X} with END tokens, resulting in a $(K + 1) \times d$ embedding matrix.

3.2 Autoregressive Group-Centric Generation

At each time step t , the model determines the next group M_t to add and establishes directed edges

from the previously generated groups $\mathcal{G}_{<t}$ to M_t .

Historical Aggregation. The model must aggregate the structural and semantic information of the current graph state. We use a gated recurrent unit (GRU) to compress the sequence of previously generated group embeddings into a historical state $\mathbf{h}_{\text{his}}^{(t)}$:

$$\mathbf{h}_{\text{his}}^{(t)} = \text{GRU}([\mathbf{x}_{M_1}, \dots, \mathbf{x}_{M_{t-1}}]). \quad (6)$$

To ensure the generation remains aligned with the task, we employ a dynamic gate $g^{(t)}$ to fuse the historical context with the task representation \mathbf{z}_Q :

$$g^{(t)} = \sigma \left(\frac{\mathbf{h}_{\text{his}}^{(t)} \cdot \mathbf{z}_Q}{\sqrt{d}} \right), \quad (7)$$

$$\mathbf{h}_{\text{comb}}^{(t)} = (1 - g^{(t)})\mathbf{h}_{\text{his}}^{(t)} + g^{(t)}\mathbf{z}_Q + \mathbf{e}_{\text{pos}}^{(t)}, \quad (8)$$

where $\mathbf{e}_{\text{pos}}^{(t)}$ is a learnable step embedding providing positional information.

Group Prediction. The fused state $\mathbf{h}_{\text{comb}}^{(t)}$ passes through a dedicated GRU to produce the raw group feature $\mathbf{x}_{\text{group}}^{(t)}$. Rather than using this raw feature directly, we pass it through the CIB layer (detailed in Section 3.3) to obtain a compressed, noise-filtered representation $\mathbf{c}_{\text{group}}^{(t)}$. The probability distribution over the candidate groups is then computed via scaled dot-product attention with the candidate matrix \mathbf{X} :

$$P(M_t | \mathcal{G}_{<t}, \mathbf{z}_Q) = \text{Softmax}(\mathbf{c}_{\text{group}}^{(t)} \mathbf{X}^T). \quad (9)$$

Edge Prediction. Once M_t is selected, the model predicts incoming edges from all existing groups $M_i \in \mathcal{G}_{<t}$. For each candidate edge (M_i, M_t) , we concatenate the historical state of the source group, the new group’s embedding, and the task representation to form the raw edge feature $\mathbf{x}_{\text{edge}}^{(i,t)} = [\mathbf{h}_{\text{comb}}^{(i)} \parallel \mathbf{x}_{M_t} \parallel \mathbf{z}_Q]$. This feature is similarly compressed by the CIB layer into $\mathbf{c}_{\text{edge}}^{(i,t)}$. A binary classifier then predicts the edge existence probability:

$$P(e_{i,t} = 1 | M_i, \mathcal{G}_{<t}, \mathbf{z}_Q) = \sigma(\text{MLP}(\mathbf{c}_{\text{edge}}^{(i,t)})). \quad (10)$$

3.3 Conditional Information Bottleneck

As the communication graph grows, the raw historical features \mathbf{x} (i.e., $\mathbf{x}_{\text{group}}^{(t)}$ or $\mathbf{x}_{\text{edge}}^{(i,t)}$) inevitably accumulate task-irrelevant signals, such as spurious group co-occurrences. To prevent this noise from propagating to the target prediction y (the next group M_t or edge $e_{i,t}$), we introduce a CIB layer. Following Eq. (4), we instantiate the condition variable as the global task representation \mathbf{z}_Q . While primarily motivated by inter-group noise filtering, we apply CIB to both group and edge predictions for architectural uniformity. The CIB extracts a compressed latent representation \mathbf{c} from \mathbf{x} by optimizing the following objective:

$$\min \mathcal{L}_{\text{CIB}} = \underbrace{-I(\mathbf{c}; y | \mathbf{z}_Q)}_{\text{Predictive Term}} + \beta \underbrace{I(\mathbf{x}; \mathbf{c} | \mathbf{z}_Q)}_{\text{Compression Term}} \quad (11)$$

Because directly computing mutual information is intractable, we derive variational upper bounds to operationalize both terms.

Minimizing Predictive Term. The first term ensures \mathbf{c} retains sufficient information to predict y . We minimize its variational upper bound using a decoder p_ψ :

$$-I(\mathbf{c}; y | \mathbf{z}_Q) \leq \mathbb{E}_{\mathbf{c} \sim q_\phi(\mathbf{c} | \mathbf{x})} [-\log p_\psi(y | \mathbf{c}, \mathbf{z}_Q)] \triangleq \mathcal{L}_{\text{task}}. \quad (12)$$

In practice, because our architecture explicitly fuses the task query \mathbf{z}_Q into the historical state \mathbf{x} prior to compression, we assume the variables form a Markov chain $\mathbf{z}_Q \rightarrow \mathbf{x} \rightarrow \mathbf{c} \rightarrow y$. Under this assumption, \mathbf{c} acts as a sufficient statistic for predicting y , rendering y conditionally independent of \mathbf{z}_Q given \mathbf{c} . Consequently, we efficiently parameterize the decoder as $p_\psi(y | \mathbf{c})$, which serves as a valid approximation of $p_\psi(y | \mathbf{c}, \mathbf{z}_Q)$ provided that the predictive term successfully forces \mathbf{c} to retain the task-relevant signals.

Minimizing Compression Term. The second term restricts the flow of noisy historical information. Unlike standard Variational IB (Alemi et al., 2017) that uses a fixed standard normal prior, we introduce a task-conditioned prior $p_\theta(\mathbf{c} | \mathbf{z}_Q)$. This conditional prior holds under the premise that different task types (e.g., math reasoning vs. code generation) inherently require different baseline topological structures, meaning the latent space of valid communication graphs is fundamentally task-dependent. We parameterize both the encoder $q_\phi(\mathbf{c} | \mathbf{x})$ and the conditional prior $p_\theta(\mathbf{c} | \mathbf{z}_Q)$ as multivariate Gaussians with diagonal covariances via MLPs. The mutual information is upper-bounded by their Kullback-Leibler (KL) divergence:

$$I(\mathbf{x}; \mathbf{c} | \mathbf{z}_Q) \leq \mathbb{E}_{\mathbf{x}, \mathbf{z}_Q} [D_{\text{KL}}(q_\phi(\mathbf{c} | \mathbf{x}) \parallel p_\theta(\mathbf{c} | \mathbf{z}_Q))] \triangleq \mathcal{L}_{\text{KL}}. \quad (13)$$

During training, we sample \mathbf{c} using the reparameterization trick:

$$\mathbf{c} = \mu_\phi(\mathbf{x}) + \sigma_\phi(\mathbf{x}) \odot \epsilon, \quad \epsilon \sim \mathcal{N}(\mathbf{0}, \mathbf{I}). \quad (14)$$

Tractable Objective. By combining these bounds, we obtain an end-to-end optimizable loss function:

$$\mathcal{L}_{\text{CIB}} \leq \mathcal{L}_{\text{task}} + \beta \mathcal{L}_{\text{KL}}. \quad (15)$$

This formulation directly bridges to our final training objective (Section 3.4), where $\mathcal{L}_{\text{task}}$ corresponds to the supervised cross-entropy losses, and \mathcal{L}_{KL} acts as a task-guided regularizer to filter structural noise.

3.4 Training and Inference Strategy

Data Construction. The autoregressive generator requires ground-truth sequences of groups and edges for supervised training. Since manually authoring optimal task-graph pairs is infeasible, we curate a training dataset $\mathcal{D} = \{(\mathcal{Q}, \mathcal{G}^*)\}$ via an automated heuristic exploration process. For a given set of training queries, we sample diverse candidate topologies \mathcal{G} by varying group combinations and edge densities. We then execute these graphs on the target tasks using the underlying LLMs. Graphs that successfully produce the correct final answer are collected. To encourage efficiency, we filter these successful graphs to retain the minimal viable topologies (i.e., those with fewer groups and edges), which serve as our positive ground-truth trajectories \mathcal{G}^* .

Training Objective. We train the model end-to-end using Teacher Forcing on the curated trajectories in \mathcal{D} , avoiding the high variance typical of on-line reinforcement learning. The total loss \mathcal{L} is the empirical realization of the CIB objective across all generation steps. Specifically, the task loss $\mathcal{L}_{\text{task}}$ is instantiated as the negative log-likelihood for group prediction ($\mathcal{L}_{\text{group}}$) and binary cross-entropy for edge prediction ($\mathcal{L}_{\text{edge}}$):

$$\mathcal{L}_{\text{group}} = -\mathbb{E}_{\mathcal{D}} \left[\sum_t \log P(M_t^* | \mathcal{G}_{<t}^*, \mathbf{z}_{\mathcal{Q}}) \right], \quad (16)$$

$$\mathcal{L}_{\text{edge}} = -\mathbb{E}_{\mathcal{D}} \left[\sum_t \sum_{i < t} \log P(e_{i,t}^* | M_i^*, \mathcal{G}_{<t}^*, \mathbf{z}_{\mathcal{Q}}) \right]. \quad (17)$$

The KL divergence regularizer \mathcal{L}_{KL} is applied at both the group and edge levels. The final joint objective is:

$$\mathcal{L} = \underbrace{\mathcal{L}_{\text{group}} + \mathcal{L}_{\text{edge}}}_{\text{Predictive Task}} + \underbrace{\beta_g \mathcal{L}_{\text{KL}}^{\text{group}} + \beta_e \mathcal{L}_{\text{KL}}^{\text{edge}}}_{\text{Information Compression}}, \quad (18)$$

where β_g and β_e control the bottleneck strength. To prevent overly strong compression before the generator learns meaningful structural patterns, we employ a KL warm-up strategy, gradually increasing the β weights during early training epochs.

Inference Procedure. During inference, given a new task query \mathcal{Q} , the trained GoAgent model generates a group-level graph autoregressively. The process, detailed in Algorithm 2, starts with the encoded task embedding and enters a generation loop. At each step, it selects a new group using the deterministic mean to bypass stochastic sampling. If the selected group is not the special END token, the model then samples the existence of incoming edges from all previously generated groups via a Bernoulli distribution. This loop continues until the END token is produced.

4 Experiments

Benchmarks. Following (Zhang et al., 2025b), we evaluate our approach on general reasoning using MMLU (Hendrycks et al., 2021), mathematical reasoning using GSM8K (Cobbe et al., 2021), MultiArith (Roy and Roth, 2015), SVAMP (Patel et al., 2021), and AQuA (Ling et al., 2017), as well as code generation using HumanEval (Chen et al., 2021). Details are provided in Appendix C.

Baselines. We compare GoAgent against three types of methods. The single-agent baselines include Vanilla (direct reasoning), Chain-of-Thought (CoT) (Wei et al., 2022) and Self-Consistency (SC) (Wang et al., 2023). For MAS with fixed topologies, we evaluate Chain, Tree, Complete graph, Random graph (Qian et al., 2025), and LLM-Debate (Du et al., 2024). For MAS with learnable topologies, we include AgentPrune (Zhang et al., 2025a), AgentDropout (Wang et al., 2025b), G-Designer (Zhang et al., 2025b), EIB-LEARNER (Shen et al., 2025), and ARG-Designer (Li et al., 2025). Further baseline details are in Appendix D.

Implementation Details. We access GPT models via the OpenAI API, primarily using gpt-4o-2024-08-06. A summarizer agent aggregates the dialogue history to produce the final solution, with the maximum interaction round set to $T = 3$ across all baselines and experiments. The group encoder uses all-MiniLM-L6-v2 (Wang et al., 2020b) with an embedding dimension of $d = 384$. Following standard LLM-MAS configurations (Zhang et al., 2025b; Li et al., 2025), we provide explicit agent profiles for multi-agent methods and use GPT-4 to generate this profile pool. For the CIB hyperparameters β_g and β_e (analyzed in Appendix E), we apply a linear warm-up strategy over the first $E_{\text{warm}} = 10$ training epochs. For all datasets, we train the model using only $B \in \{40, 60\}$ queries. Additional implementation details are in Appendix F.

4.1 Performance Comparison

Table 1 shows that GoAgent achieves consistent state-of-the-art accuracy across all six benchmarks. Compared to node-centric autoregressive methods like ARG-Designer and template-based pruning methods like EIB-LEARNER, GoAgent shows larger gains on complex reasoning tasks, such as MMLU (1.96% \uparrow) and HumanEval (2.47% \uparrow). These improvements on harder tasks support our core motivation: constructing topologies at the group level leverages cohesive expert clusters, such as a solver paired with a verifier. This avoids the disjointed workflows and missing inter-role connections common in node-centric generation.

4.2 Ablation Study

We conduct ablation studies to isolate the contributions of key components in GoAgent, with results detailed in Table 2. We evaluate three variants:

Table 1: Overall performance comparison on six benchmarks (%). The best results are highlighted in **bold**.

Method	MMLU	GSM8K	AQuA	MultiArith	SVAMP	HumanEval	Avg.
Vanilla	80.39	82.30	71.06	93.09	86.55	71.39	80.80
CoT	81.69 \uparrow 1.30	86.50 \uparrow 4.20	73.58 \uparrow 2.52	93.25 \uparrow 0.16	87.36 \uparrow 0.81	74.67 \uparrow 3.28	82.84 \uparrow 2.05
SC	83.66 \uparrow 3.27	81.60 \downarrow 0.70	75.63 \uparrow 4.57	94.12 \uparrow 1.03	88.59 \uparrow 2.04	79.83 \uparrow 8.44	83.91 \uparrow 3.11
Chain	83.01 \uparrow 2.62	88.30 \uparrow 6.00	74.05 \uparrow 2.99	93.27 \uparrow 0.18	87.17 \uparrow 0.62	81.37 \uparrow 9.98	84.53 \uparrow 3.73
Tree	81.04 \uparrow 0.65	85.20 \uparrow 2.90	71.23 \uparrow 0.17	93.68 \uparrow 0.59	88.91 \uparrow 2.36	80.53 \uparrow 9.14	83.43 \uparrow 2.64
Complete	82.35 \uparrow 1.96	80.10 \downarrow 2.20	72.95 \uparrow 1.89	94.53 \uparrow 1.44	84.01 \downarrow 2.54	79.03 \uparrow 7.64	82.16 \uparrow 1.37
Random	84.31 \uparrow 3.92	86.90 \uparrow 4.60	76.48 \uparrow 5.42	94.08 \uparrow 0.99	87.54 \uparrow 0.99	82.66 \uparrow 11.27	85.33 \uparrow 4.53
LLM-Debate	84.96 \uparrow 4.57	91.40 \uparrow 9.10	77.65 \uparrow 6.59	96.36 \uparrow 3.27	90.11 \uparrow 3.56	84.70 \uparrow 13.31	87.53 \uparrow 6.73
AgentPrune	85.07 \uparrow 4.68	91.10 \uparrow 8.80	80.51 \uparrow 9.45	94.65 \uparrow 1.56	90.58 \uparrow 4.03	86.75 \uparrow 15.36	88.11 \uparrow 7.31
AgentDropout	85.62 \uparrow 5.23	91.70 \uparrow 9.40	80.94 \uparrow 9.88	95.60 \uparrow 2.51	91.04 \uparrow 4.49	85.98 \uparrow 14.59	88.48 \uparrow 7.68
G-Designer	86.92 \uparrow 6.53	93.80 \uparrow 11.50	81.60 \uparrow 10.54	96.50 \uparrow 3.41	93.10 \uparrow 6.55	88.33 \uparrow 16.94	90.04 \uparrow 9.25
EIB-LEARNER	88.90 \uparrow 8.51	95.20 \uparrow 12.90	83.46 \uparrow 12.40	96.83 \uparrow 3.74	94.70 \uparrow 8.15	89.15 \uparrow 17.76	91.37 \uparrow 10.58
ARG-Designer	89.54 \uparrow 9.15	94.37 \uparrow 12.07	85.51 \uparrow 14.45	98.93 \uparrow 5.84	95.63 \uparrow 9.08	91.74 \uparrow 20.35	92.62 \uparrow 11.82
GoAgent (Ours)	91.50 \uparrow 11.11	95.30 \uparrow 13.00	86.45 \uparrow 15.39	99.11 \uparrow 6.02	96.46 \uparrow 9.91	94.21 \uparrow 22.82	93.84 \uparrow 13.04

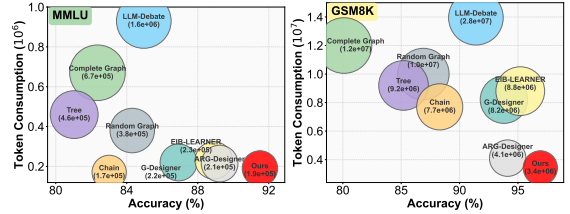
Table 2: Ablation study of GoAgent components.

Model	MMLU	GSM8K	HumanEval	Avg.
Vanilla	80.39	82.30	71.39	78.03
GoAgent	91.50	95.30	94.21	93.67
w/o Group	88.89	93.75	91.74	91.46
w/o CIB	88.23	93.96	92.56	91.58
w/o ALL	86.92	91.16	90.56	89.55

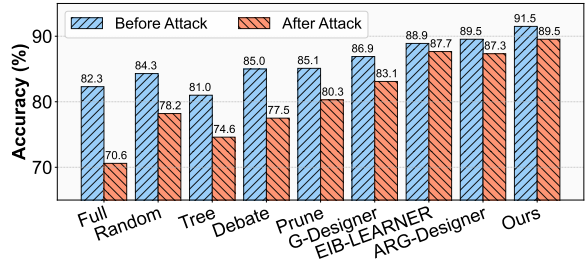
(1) the w/o CIB variant removes the Conditional Information Bottleneck layer, forcing the model to rely on uncompressed historical features; (2) the w/o Group variant replaces group-level candidates with individual agent roles, reverting to a node-centric generation paradigm; and (3) the w/o ALL variant removes both mechanisms. Removing either component leads to clear performance drops. For instance, the w/o Group variant suffers a **2.61%** accuracy decrease on MMLU, confirming that implicit coordination through node-level generation struggles with complex tasks. Similarly, the w/o CIB variant experiences a **3.27%** drop on MMLU. Without noise compression, the system becomes vulnerable to irrelevant historical signals, which misguide the edge prediction module into forming spurious connections. Together, these findings show that group-level generation and structural noise filtering are highly complementary.

4.3 Token Efficiency

A key motivation for moving beyond node-centric generation is to reduce inference-time communication overhead. Figures 3a and 3b report the total LLM inference tokens on MMLU and GSM8K.



(a) Token cost on MMLU. (b) Token cost on GSM8K.



(c) Robustness under attack.

Figure 3: Experiments on token consumption and robustness against prompt injection attacks.

Dense topologies like Complete graphs and LLM-Debate consume excessive tokens due to unrestricted information exchange. Although ARG-Designer learns sparse structures, its node-centric approach still yields unnecessary point-to-point connections. In contrast, GoAgent reduces token consumption by **17%** compared to the SOTA baseline, while maintaining high accuracy. By treating cohesive groups as atomic blocks and using the CIB layer to filter irrelevant inter-group edges, the model avoids redundant agent-level connections. This allows GoAgent to maintain a token footprint comparable to simple trees while achieving the performance of highly expressive topologies.

4.4 Robustness Analysis

Following (Zhuge et al., 2024), we simulate a system prompt attack by injecting adversarial prompts into a single agent. As illustrated in Figure 3c, node-centric methods such as G-Designer and ARG-Designer suffer sharp performance drops under these attacks, because local errors rapidly propagate through their networks. In contrast, GoAgent shows significantly better robustness, maintaining an accuracy of **89.54%**. This resilience stems from the CIB layer, which acts as a filter by compressing incoming features conditioned on the task representation. Through this mechanism, the model learns to identify and discard signals that deviate from the task goal, thereby restricting the spread of localized hallucinations across group boundaries.

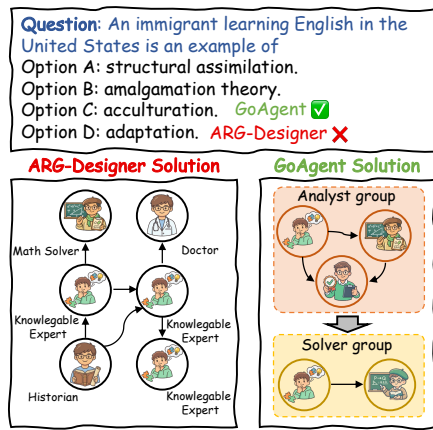


Figure 4: Cases of ARG-Designer and GoAgent.

4.5 Case Study

To further illustrate the advantages of GoAgent over learning-based baselines like ARG-Designer, we conduct a comparative case study on representative MMLU examples, shown in Figure 4. The main difference lies in the redundancy of composition and link generation. Without explicit higher-order constraints, ARG-Designer tends to connect redundant agents, and the density of its generated graphs increases sharply with task complexity. GoAgent instead selects groups and inter-group links from an explicitly constructed pool, reducing unnecessary communication. Consequently, GoAgent constructs more efficient collaboration graphs with fewer agents and messages, lowering token usage without sacrificing accuracy.

5 Related Work

LLM-based Multi-Agent Systems. MAS coordinate diverse roles to solve complex tasks (Zhang

et al., 2024a; Yao et al., 2023; Tran et al., 2025), and their performance depends heavily on the underlying communication topology. Early architectures relied on static structures such as chains (Zhang et al., 2024b; Zhou et al., 2024). To enable adaptive communication, template-based methods like G-Designer, AgentPrune, and AgentDropout (Zhang et al., 2025b,a; Wang et al., 2025b; Shen et al., 2025; Jiang et al., 2025; Wu et al., 2026) optimize topologies by pruning predefined graphs. More recently, ARG-Designer (Li et al., 2025) bypassed template constraints entirely by autoregressively constructing topologies from scratch. However, all these methods operate at the node level, treating individual agents as atomic units. This node-centric paradigm has difficulty capturing cohesive collaborative structures and frequently generates redundant edges.

Group-Aware Graph Generation. Node-centric graph generation often faces scalability and structural coherence challenges. To overcome these limitations, research in graph representation learning has explored higher-order paradigms. Hierarchical networks (Jin et al., 2020; Karami, 2023) explicitly model macroscopic subgraphs before establishing microscopic connections. Diffusion-based methods (Liu et al., 2024; Xu and Ma, 2025) incorporate global and local constraints to ensure structural validity, and scalable frameworks (Liu and Sariyüce, 2023; Sarpe et al., 2024) demonstrate that generating graphs through higher-order units improves both efficiency and fidelity. Drawing on these principles, GoAgent introduces a group-centric paradigm to MAS. By using LLM-derived collaborative groups as atomic building blocks, it preserves intra-group cohesion and simplifies inter-group coordination.

6 Conclusion

In this paper, we present GoAgent, a communication topology generation method for LLM-based multi-agent systems, driven by a group-centric design paradigm. By treating collaborative groups as atomic generative units and using a CIB to compress historical signals, GoAgent adaptively forms task-specific topologies while suppressing task-irrelevant noise. Experiments across six benchmarks show that GoAgent consistently achieves state-of-the-art accuracy, improves structural robustness, and reduces communication overhead.

Limitations

Although our method demonstrates strong performance and efficiency across reasoning and coding benchmarks, several limitations remain. First, our approach relies on a predefined pool of collaborative groups generated offline by an LLM. While this significantly reduces the search space and ensures intra-group cohesion, it inherently constrains the model’s flexibility; specifically, GoAgent cannot dynamically synthesize entirely novel group structures or roles during inference if a task requires expertise outside the predefined pool. Second, our current evaluation primarily focuses on static reasoning tasks (e.g., MMLU, GSM8K). The effectiveness of group-centric topology generation in highly dynamic, interactive environments, including embodied AI or multi-agent reinforcement learning, remains to be thoroughly investigated in future research.

Ethics Statement

Our research focuses on scientific questions and does not involve human subjects, animals, or environmentally sensitive materials. We foresee no ethical risks or conflicts of interest. We are committed to maintaining scientific integrity and ethics to ensure the validity and reliability of our findings.

References

- Alexander A Alemi, Ian Fischer, Joshua V Dillon, and Kevin Murphy. 2017. Deep variational information bottleneck. In *International Conference on Learning Representations*.
- Daniel Barkoczi and Mirta Galesic. 2016. Social learning strategies modify the effect of network structure on group performance. *Nature communications*, 7(1):13109.
- Lorenzo Betti, Luca Gallo, Johannes Wachs, and Federico Battiston. 2025. The dynamics of leadership and success in software development teams. *Nature Communications*, 16(1):3956.
- Mark Chen, Jerry Tworek, Heewoo Jun, Qiming Yuan, Henrique Ponde De Oliveira Pinto, Jared Kaplan, Harri Edwards, Yuri Burda, Nicholas Joseph, Greg Brockman, and 1 others. 2021. Evaluating large language models trained on code. *arXiv preprint arXiv:2107.03374*.
- Karl Cobbe, Vineet Kosaraju, Mohammad Bavarian, Mark Chen, Heewoo Jun, Lukasz Kaiser, Matthias Plappert, Jerry Tworek, Jacob Hilton, Reiichiro Nakano, and 1 others. 2021. Training verifiers to solve math word problems. *arXiv preprint arXiv:2110.14168*.
- Yilun Du, Shuang Li, Antonio Torralba, Joshua B Tenenbaum, and Igor Mordatch. 2024. Improving factuality and reasoning in language models through multiagent debate. In *Forty-first international conference on machine learning*.
- David Gondek and Thomas Hofmann. 2003. Conditional information bottleneck clustering. In *3rd ieee international conference on data mining, workshop on clustering large data sets*, pages 36–42.
- Xudong Guo, Kaixuan Huang, Jiale Liu, Wenhui Fan, Natalia Vélez, Qingyun Wu, Huazheng Wang, Thomas L Griffiths, and Mengdi Wang. 2026. Embodied llm agents learn to cooperate in organized teams. *IEEE Transactions on Computational Social Systems*.
- Dan Hendrycks, Collin Burns, Steven Basart, Andy Zou, Mantas Mazeika, Dawn Song, and Jacob Steinhardt. 2021. Measuring massive multitask language understanding. In *International Conference on Learning Representations*.
- Shengchao Hu, Li Shen, Ya Zhang, and Dacheng Tao. 2024. Learning multi-agent communication from graph modeling perspective. In *The Twelfth International Conference on Learning Representations*.
- Eric Hanchen Jiang, Guancheng Wan, Sophia Yin, Mengting Li, Yuchen Wu, Xiao Liang, Xinfeng Li, Yizhou Sun, Wei Wang, Kai-Wei Chang, and 1 others. 2025. Dynamic generation of multi-llm agents communication topologies with graph diffusion models. *arXiv preprint arXiv:2510.07799*.
- Wengong Jin, Regina Barzilay, and Tommi Jaakkola. 2020. Hierarchical generation of molecular graphs using structural motifs. In *International conference on machine learning*, pages 4839–4848. PMLR.
- Mahdi Karami. 2023. Higen: Hierarchical graph generative networks. In *The Twelfth International Conference on Learning Representations*.
- Shiyuan Li, Yixin Liu, Qingsong Wen, Chengqi Zhang, and Shirui Pan. 2025. Assemble your crew: Automatic multi-agent communication topology design via autoregressive graph generation. *arXiv preprint arXiv:2507.18224*.
- Tian Liang, Zhiwei He, Wenxiang Jiao, Xing Wang, Yan Wang, Rui Wang, Yujiu Yang, Shuming Shi, and Zhaopeng Tu. 2024. Encouraging divergent thinking in large language models through multi-agent debate. In *Proceedings of the 2024 conference on empirical methods in natural language processing*, pages 17889–17904.
- Wang Ling, Dani Yogatama, Chris Dyer, and Phil Blunsom. 2017. Program induction by rationale generation: Learning to solve and explain algebraic word

- problems. In *Proceedings of the 55th annual meeting of the association for computational linguistics (volume 1: Long papers)*, pages 158–167.
- Gang Liu, Jiaxin Xu, Tengfei Luo, and Meng Jiang. 2024. Graph diffusion transformers for multi-conditional molecular generation. *Advances in Neural Information Processing Systems*, 37:8065–8092.
- Penghang Liu and Ahmet Erdem Sariyüce. 2023. Using motif transitions for temporal graph generation. In *Proceedings of the 29th ACM SIGKDD conference on knowledge discovery and data mining*, pages 1501–1511.
- Yixin Liu, Guibin Zhang, Kun Wang, Shiyuan Li, and Shirui Pan. 2025. Graph-augmented large language model agents: Current progress and future prospects. *arXiv preprint arXiv:2507.21407*.
- Arkil Patel, Satwik Bhattamishra, and Navin Goyal. 2021. Are nlp models really able to solve simple math word problems? In *Proceedings of the 2021 conference of the North American chapter of the association for computational linguistics: human language technologies*, pages 2080–2094.
- Niccolò Pescetelli, Alex Rutherford, and Iyad Rahwan. 2021. Modularity and composite diversity affect the collective gathering of information online. *Nature Communications*, 12(1):3195.
- Chen Qian, Zihao Xie, YiFei Wang, Wei Liu, Kunlun Zhu, Hanchen Xia, Yufan Dang, Zhuoyun Du, Weize Chen, Cheng Yang, and 1 others. 2025. Scaling large language model-based multi-agent collaboration. In *The Thirteenth International Conference on Learning Representations*.
- Michael Rizvi-Martel, Satwik Bhattamishra, Neil Rathi, Guillaume Rabusseau, and Michael Hahn. 2026. Benefits and limitations of communication in multi-agent reasoning. In *The Fourteenth International Conference on Learning Representations*.
- Subhro Roy and Dan Roth. 2015. Solving general arithmetic word problems. In *Proceedings of the 2015 conference on empirical methods in natural language processing*, pages 1743–1752.
- Ilie Sarpe, Fabio Vandin, and Aristides Gionis. 2024. Scalable temporal motif densest subnetwork discovery. In *Proceedings of the 30th ACM SIGKDD Conference on Knowledge Discovery and Data Mining*, pages 2536–2547.
- Xu Shen, Yixin Liu, Yiwei Dai, Yili Wang, Rui Miao, Yue Tan, Shirui Pan, and Xin Wang. 2025. Understanding the information propagation effects of communication topologies in llm-based multi-agent systems. In *Proceedings of the 2025 Conference on Empirical Methods in Natural Language Processing*, pages 12358–12372.
- Naftali Tishby, Fernando C Pereira, and William Bialek. 2000. The information bottleneck method. *arXiv preprint physics/0004057*.
- Naftali Tishby and Noga Zaslavsky. 2015. Deep learning and the information bottleneck principle. In *2015 IEEE information theory workshop (itw)*, pages 1–5. Ieee.
- Khanh-Tung Tran, Dung Dao, Minh-Duong Nguyen, Quoc-Viet Pham, Barry O’Sullivan, and Hoang D Nguyen. 2025. Multi-agent collaboration mechanisms: A survey of llms. *arXiv preprint arXiv:2501.06322*.
- Haochun Wang, Sendong Zhao, Jingbo Wang, Zewen Qiang, Bing Qin, and Ting Liu. 2025a. Beyond frameworks: Unpacking collaboration strategies in multi-agent systems. In *Proceedings of the 63rd Annual Meeting of the Association for Computational Linguistics (Volume 1: Long Papers)*, pages 21361–21375.
- Rundong Wang, Xu He, Runsheng Yu, Wei Qiu, Bo An, and Zinovi Rabinovich. 2020a. Learning efficient multi-agent communication: An information bottleneck approach. In *International conference on machine learning*, pages 9908–9918. PMLR.
- Wenhui Wang, Furu Wei, Li Dong, Hangbo Bao, Nan Yang, and Ming Zhou. 2020b. Minilm: Deep self-attention distillation for task-agnostic compression of pre-trained transformers. *Advances in neural information processing systems*, 33:5776–5788.
- Xuezhi Wang, Jason Wei, Dale Schuurmans, Quoc V Le, Ed H Chi, Sharan Narang, Aakanksha Chowdhery, and Denny Zhou. 2023. Self-consistency improves chain of thought reasoning in language models. In *The Eleventh International Conference on Learning Representations*.
- Zhexuan Wang, Yutong Wang, Xuebo Liu, Liang Ding, Miao Zhang, Jie Liu, and Min Zhang. 2025b. Agentdropout: Dynamic agent elimination for token-efficient and high-performance llm-based multi-agent collaboration. In *Proceedings of the 63rd Annual Meeting of the Association for Computational Linguistics*, pages 24013–24035.
- Jason Wei, Xuezhi Wang, Dale Schuurmans, Maarten Bosma, Fei Xia, Ed Chi, Quoc V Le, Denny Zhou, and 1 others. 2022. Chain-of-thought prompting elicits reasoning in large language models. *Advances in neural information processing systems*, 35:24824–24837.
- Qingyun Wu, Gagan Bansal, Jieyu Zhang, Yiran Wu, Beibin Li, Erkang Zhu, Li Jiang, Xiaoyun Zhang, Shaokun Zhang, Jiale Liu, and 1 others. 2024. Autogen: Enabling next-gen llm applications via multi-agent conversations. In *First conference on language modeling*.
- Xingjian Wu, Xvyuan Liu, Junkai Lu, Siyuan Wang, Yang Shu, Jilin Hu, Chenjuan Guo, and Bin Yang. 2026. St-evo: Towards generative spatio-temporal evolution of multi-agent communication topologies. *arXiv preprint arXiv:2602.14681*.

- Yuwei Xu and Chenhao Ma. 2025. Modiff-graph generation with motif-aware diffusion model. In *Proceedings of the 31st ACM SIGKDD Conference on Knowledge Discovery and Data Mining V. 2*, pages 3437–3448.
- Shunyu Yao, Jeffrey Zhao, Dian Yu, Nan Du, Izhak Shafran, Karthik R Narasimhan, and Yuan Cao. 2023. React: Synergizing reasoning and acting in language models. In *The eleventh international conference on learning representations*.
- Haonan Yuan, Qingyun Sun, Xingcheng Fu, Cheng Ji, and Jianxin Li. 2024. Dynamic graph information bottleneck. In *Proceedings of the ACM Web Conference 2024*, pages 469–480.
- Guibin Zhang, Yanwei Yue, Zhixun Li, Sukwon Yun, Guancheng Wan, Kun Wang, Dawei Cheng, Jeffrey Xu Yu, and Tianlong Chen. 2025a. Cut the crap: An economical communication pipeline for llm-based multi-agent systems. In *The Thirteenth International Conference on Learning Representations*.
- Guibin Zhang, Yanwei Yue, Xiangguo Sun, Guancheng Wan, Miao Yu, Junfeng Fang, Kun Wang, Tianlong Chen, and Dawei Cheng. 2025b. G-designer: Architecting multi-agent communication topologies via graph neural networks. In *International Conference on Machine Learning*, pages 76678–76692.
- Kechi Zhang, Jia Li, Ge Li, Xianjie Shi, and Zhi Jin. 2024a. Codeagent: Enhancing code generation with tool-integrated agent systems for real-world relevel coding challenges. In *Proceedings of the 62nd Annual Meeting of the Association for Computational Linguistics*, pages 13643–13658.
- Yusen Zhang, Ruoxi Sun, Yanfei Chen, Tomas Pfister, Rui Zhang, and Sercan Arik. 2024b. Chain of agents: Large language models collaborating on long-context tasks. *Advances in Neural Information Processing Systems*, 37:132208–132237.
- Andy Zhou, Kai Yan, Michal Shlapentokh-Rothman, Haohan Wang, and Yu-Xiong Wang. 2024. Language agent tree search unifies reasoning, acting, and planning in language models. In *Proceedings of the 41st International Conference on Machine Learning*, pages 62138–62160.
- Han Zhou, Xingchen Wan, Ruoxi Sun, Hamid Palangi, Shariq Iqbal, Ivan Vulić, Anna Korhonen, and Sercan O Arik. 2026a. Multi-agent design: Optimizing agents with better prompts and topologies. In *The Fourteenth International Conference on Learning Representations*.
- Jialong Zhou, Lichao Wang, and Xiao Yang. 2026b. Guardian: Safeguarding llm multi-agent collaborations with temporal graph modeling. In *The Thirtieth Annual Conference on Neural Information Processing Systems*.
- Mingchen Zhuge, Wenyi Wang, Louis Kirsch, Francesco Faccio, Dmitrii Khizbullin, and Jürgen Schmidhuber. 2024. Gptswarm: Language agents as optimizable graphs. In *Forty-first International Conference on Machine Learning*.

A More Related Work

Information Bottleneck in Graph Learning.

The IB principle (Tishby and Zaslavsky, 2015; Alemi et al., 2017) extracts minimal sufficient statistics for a task, balancing compression and prediction. In graph learning, IB optimizes communication efficiency by minimizing message entropy (Wang et al., 2020a) or dynamically pruning redundant messages (Yuan et al., 2024). Recently, IB has been applied to LLM-based MAS; for example, GUARDIAN (Zhou et al., 2026b) compresses temporal interaction graphs to mitigate hallucination and error propagation. Building on this, GoAgent extends IB to the generative process of MAS topologies. We introduce a Conditional IB that dynamically conditions compression on the task representation, actively filtering out redundant historical communication noise as the topology expands.

B Algorithm and Complexity Analysis

The complete training procedure of GoAgent is summarized in Algorithm 1, and the inference procedure is detailed in Algorithm 2. During inference, we bypass the stochastic sampling of the CIB layer and directly use the deterministic mean $\mathbf{c} = \mu_\phi(\mathbf{x})$ for both group and edge predictions.

Time Complexity. Let T be the total number of generated groups, K be the candidate pool size, and d be the hidden dimension. At each step t , the group prediction involves GRU state updates and attention over K candidates, taking $\mathcal{O}(d^2 + Kd)$ operations. The edge prediction evaluates connections from all $t - 1$ previous groups, taking $\mathcal{O}(t \cdot d^2)$ operations. Summing over T steps, the total time complexity for graph generation is $\mathcal{O}(Td^2 + TKd + T^2d^2) = \mathcal{O}(T^2d^2 + TKd)$. Because the generation is performed at the macroscopic group level rather than the microscopic agent level, both T (typically < 3) and K (e.g., 16) are extremely small. Consequently, the computational overhead of the generator is negligible compared to the inference cost of the underlying LLMs executing the task.

Space Complexity. The learnable parameters of the generator consist solely of lightweight GRUs, MLPs, and CIB projection layers, all bounded by $\mathcal{O}(d^2)$. The candidate group embeddings require $\mathcal{O}(Kd)$ memory. Thus, the total space complexity is $\mathcal{O}(d^2 + Kd)$, making the generator highly

parameter-efficient and easy to integrate alongside large language models.

C Dataset Details

We present the dataset statistics in Table 3, following the same experimental setup as G-Designer (Zhang et al., 2025b). We evaluate GoAgent on six diverse benchmarks spanning multiple reasoning domains.

D Baseline Details

Single-Agent Methods. We compare against three single-agent baselines: (1) **Vanilla**: Direct prompting without reasoning enhancement. (2) **Chain-of-Thought (CoT)** (Wei et al., 2022): Prompts the LLM to generate intermediate reasoning steps with “Let’s think step by step”. (3) **Self-Consistency (SC)** (Wang et al., 2023): Samples five reasoning paths using CoT and selects the most consistent answer through majority voting.

Fixed Multi-Agent Topologies. We evaluate five hand-crafted topologies: (1) **Chain**: Sequential linear chain $A_1 \rightarrow A_2 \rightarrow \dots \rightarrow A_n$. (2) **Tree**: Hierarchical structure with multiple layers culminating in a root agent. (3) **Complete**: Fully connected graph enabling maximum information sharing. (4) **Random**: Randomly generated topology with random role assignments. (5) **LLM-Debate**: Debate-based topology where agents critique each other’s reasoning over multiple rounds.

Learning-Based Topology Design. We compare against five state-of-the-art learning-based methods, each trained separately per dataset: (1) **Agent-Prune** (Zhang et al., 2025a): Identifies and addresses communication redundancy by performing one-shot pruning on spatial-temporal message-passing graphs, yielding token-economic topologies while defending against adversarial attacks. (2) **Agent-Dropout** (Wang et al., 2025b): Inspired by dynamic role adjustment in management theory, identifies redundant agents and communications across different rounds by optimizing adjacency matrices, eliminating them to enhance token efficiency and task performance. (3) **G-Designer** (Zhang et al., 2025b): Employs a variational graph auto-encoder to encode agents and task-specific virtual nodes, dynamically designing task-adaptive communication topologies customized for each task’s difficulty and requirements. (4) **EIB-LEARNER** (Shen et al., 2025): Uses a

Algorithm 1 Training Procedure of GoAgent

Require: Training dataset $\mathcal{D} = \{(\mathcal{Q}, \mathcal{G}^*)\}$ curated via heuristic exploration, Total epochs E , Warm-up epochs E_{warm}

Ensure: Optimized model parameters

```
1: for epoch  $e = 1$  to  $E$  do
2:   /* Update CIB Bottleneck Strength */
3:   Compute  $\beta_g, \beta_e$  based on warm-up schedule (e.g., linear increase if  $e < E_{\text{warm}}$ )
4:   for each batch  $(\mathcal{Q}, \mathcal{G}^*) \in \mathcal{D}$  do
5:     Encode task query:  $\mathbf{z}_{\mathcal{Q}} \leftarrow \text{TaskEncoder}(\mathcal{Q})$ 
6:     Initialize batch losses:  $\mathcal{L}_{\text{group}} \leftarrow 0, \mathcal{L}_{\text{edge}} \leftarrow 0, \mathcal{L}_{\text{KL}}^{\text{group}} \leftarrow 0, \mathcal{L}_{\text{KL}}^{\text{edge}} \leftarrow 0$ 
7:     for step  $t = 1$  to  $|\mathcal{M}^*|$  do
8:       /* Teacher Forcing with Ground-Truth History */
9:       Aggregate history  $\mathbf{h}_{\text{his}}^{(t)}$  using ground-truth sequence  $\mathcal{M}_{<t}^*$ 
10:      Fuse with task  $\mathbf{z}_{\mathcal{Q}}$  to obtain  $\mathbf{h}_{\text{comb}}^{(t)}$  via Eq. (7) and Eq. (8)
11:      /* Group CIB & Prediction Loss */
12:      Extract raw group feature  $\mathbf{x}_{\text{group}}^{(t)}$ 
13:      Sample  $\mathbf{c}_{\text{group}}^{(t)}$  using the reparameterization trick via Eq. (14)
14:      Accumulate  $\mathcal{L}_{\text{group}}$  via Eq. (16)
15:      Accumulate  $\mathcal{L}_{\text{KL}}^{\text{group}}$  based on expected KL divergence
16:      /* Edge CIB & Prediction Loss */
17:      for each existing group  $M_i^* \in \mathcal{M}_{<t}^*$  do
18:        Construct raw edge feature  $\mathbf{x}_{\text{edge}}^{(i,t)} = [\mathbf{h}_{\text{comb}}^{(i,t)} \parallel \mathbf{x}_{M_i^*} \parallel \mathbf{z}_{\mathcal{Q}}]$ 
19:        Sample  $\mathbf{c}_{\text{edge}}^{(i,t)}$  using the reparameterization trick via Eq. (14)
20:        Compute  $p_{i,t}$  via Eq. (10)
21:        Accumulate  $\mathcal{L}_{\text{edge}}$  via Eq. (17)
22:        Accumulate  $\mathcal{L}_{\text{KL}}^{\text{edge}}$  based on expected KL divergence
23:      end for
24:    end for
25:    /* Optimization */
26:    Compute total loss  $\mathcal{L}$  via Eq. (18)
27:    Update parameters using gradient descent on  $\mathcal{L}$ 
28:  end for
29: end for
30: return Optimized parameters
```

Table 3: Dataset descriptions and statistics.

Category	Dataset	Answer Type	Metric	#Test	License
General reasoning	MMLU	Multi-choice	Acc.	153	MIT License
	GSM8K	Number	Acc.	1,319	MIT License
Math reasoning	MultiArith	Number	Acc.	600	Unspecified
	SVAMP	Number	Acc.	1,000	MIT License
	AQuA	Multi-choice	Acc.	254	Apache-2.0
Code generation	HumanEval	Code	Pass@1	164	MIT License

causal framework to analyze error propagation patterns and designs topologies by fusing connectivity patterns from both dense and sparse graphs, balanc-

ing error suppression with beneficial information diffusion. (5) **ARG-Designer** (Li et al., 2025): Autoregressively constructs communication topolo-

Algorithm 2 Inference Procedure of GoAgent

Require: Task query \mathcal{Q} , Candidate group embeddings $\mathbf{X} \in \mathbb{R}^{(K+1) \times d}$

Ensure: Group-level communication graph $\mathcal{G} = (\mathcal{M}, \mathcal{E})$

- 1: **Initialize:** $\mathcal{M} \leftarrow \emptyset, \mathcal{E} \leftarrow \emptyset, t \leftarrow 1$
- 2: Encode task query to global representation: $\mathbf{z}_{\mathcal{Q}} \leftarrow \text{TaskEncoder}(\mathcal{Q})$
- 3: **while** True **do**
- 4: /* 1. Historical Aggregation */
- 5: Aggregate history $\mathbf{h}_{\text{his}}^{(t)} \leftarrow \text{GRU}([\mathbf{x}_{M_1}, \dots, \mathbf{x}_{M_{t-1}}])$
- 6: Compute dynamic gate $g^{(t)}$ and fused state $\mathbf{h}_{\text{comb}}^{(t)}$ via Eq. (7) and Eq. (8)
- 7: /* 2. Group Prediction */
- 8: Extract raw group feature $\mathbf{x}_{\text{group}}^{(t)}$ from $\mathbf{h}_{\text{comb}}^{(t)}$ via GRU
- 9: Compress feature using deterministic CIB mean: $\mathbf{c}_{\text{group}}^{(t)} \leftarrow \mu_{\phi}(\mathbf{x}_{\text{group}}^{(t)})$
- 10: Compute probability distribution over candidates $P(M_t)$ via Eq. (9)
- 11: Sample next group $M_t = \arg \max P(M_t)$
- 12: **if** $M_t == \text{END}$ **then**
- 13: **break**
- 14: **end if**
- 15: Add group to graph: $\mathcal{M} \leftarrow \mathcal{M} \cup \{M_t\}$
- 16: /* 3. Edge Prediction */
- 17: **for** each existing group $M_i \in \mathcal{M}_{<t}$ **do**
- 18: Construct raw edge feature: $\mathbf{x}_{\text{edge}}^{(i,t)} = [\mathbf{h}_{\text{comb}}^{(i)} \parallel \mathbf{x}_{M_i} \parallel \mathbf{z}_{\mathcal{Q}}]$
- 19: Compress feature using deterministic CIB mean: $\mathbf{c}_{\text{edge}}^{(i,t)} \leftarrow \mu_{\phi}(\mathbf{x}_{\text{edge}}^{(i,t)})$
- 20: Predict edge probability $p_{i,t}$ via Eq. (10)
- 21: Sample $a_{i,t} \sim \text{Bernoulli}(p_{i,t})$
- 22: **if** $a_{i,t} = 1$ **then**
- 23: $\mathcal{E} \leftarrow \mathcal{E} \cup \{(M_i, M_t)\}$
- 24: **end if**
- 25: **end for**
- 26: **if** no edge was added for M_t **then**
- 27: $i^* \leftarrow \arg \max_i p_{i,t}; \quad \mathcal{E} \leftarrow \mathcal{E} \cup \{(M_{i^*}, M_t)\}$
- 28: **end if**
- 29: $t \leftarrow t + 1$
- 30: **end while**
- 31: **return** $\mathcal{G} = (\mathcal{M}, \mathcal{E})$

gies from scratch by sequentially adding individual agents with task-specific role assignments and establishing pairwise connections, bypassing the need for predefined template graphs.

E Parameter Sensitivity Analysis

The Conditional Information Bottleneck (CIB) is governed by two key hyperparameters: β_g and β_e , which control the strength of the KL divergence penalty during group prediction and edge prediction, respectively. We investigate the sensitivity of GoAgent to these parameters on the MMLU dataset.

As illustrated in Figure 5, the model’s perfor-

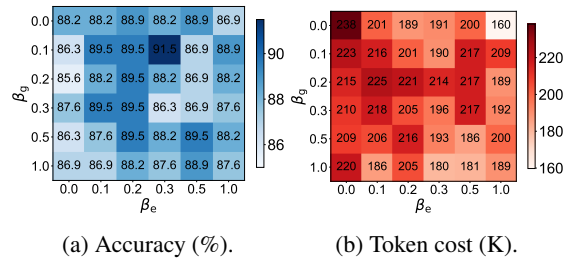


Figure 5: Heatmap of model performance with varying β_g and β_e on the MMLU dataset.

mance is highly sensitive to the bottleneck strength. Setting β too low (e.g., $\beta_e = 0.0$) renders the bottleneck ineffective, allowing historical noise to pass

through and resulting in over-connected graphs with high token costs and lower accuracy. Conversely, setting β too high (e.g., $\beta_e > 0.5$) forces the model to aggressively compress the features, discarding necessary historical context and leading to under-connected, poorly coordinated topologies.

Interestingly, the optimal configuration occurs in a highly asymmetric region ($\beta_g \approx 0.0$ and $\beta_e \approx 0.3$). This indicates that edge prediction benefits significantly more from compression than group prediction. This asymmetry aligns with our intuition: determining *which* group to generate next (group prediction) requires full access to the rich historical context to avoid duplicating roles. However, determining *how* these groups connect (edge prediction) is highly susceptible to the redundant connectivity patterns common in prior generative models. The CIB layer effectively filters out this structural noise, ensuring that edges are formed only when task-relevant information must be routed between groups.

F Implementation Details

Training. During the heuristic exploration described in Section 3.4, candidate topologies are drawn from three structural families: Chain, Star, and FullConnected. We train with AdamW (learning rate 1×10^{-4} , weight decay 1×10^{-3} , gradient clipping 1.0) for $E = 100$ epochs with a batch size of 40. The CIB bottleneck strength undergoes linear warm-up over the first $E_{\text{warm}} = 10$ epochs. Notably, only $B \in \{40, 60\}$ training queries per dataset suffice, because the generator learns *structural collaboration patterns* (which group types co-occur and how they connect) rather than task-specific reasoning, which is handled entirely by the underlying LLMs.

Architecture. All modules use hidden dimension $h = 256$. The task encoder FFN projects $d \rightarrow h \rightarrow d$ with ReLU. The historical aggregation GRU, group prediction GRU, and edge prediction GRU are each single-layer with input and hidden size d . For edge prediction, the concatenated feature $\mathbf{x}_{\text{edge}}^{(i,t)} \in \mathbb{R}^{3d}$ is projected via a two-layer MLP ($3d \rightarrow h \rightarrow d$, ReLU), processed by the edge GRU, then passed through the CIB layer. The final edge classification head maps $d \rightarrow h \rightarrow 1$ with sigmoid output. During inference, edges are sampled via Bernoulli; if no edge is sampled for a newly added group, the highest-probability edge is added to guarantee connectivity.

F.1 LLM Prompt Templates

We use GPT-4o with temperature 0.7 to generate diverse (query, topology) pairs. The system prompt instructs the LLM to generate queries spanning multiple domains (code implementation, mathematical reasoning, multiple-choice questions, knowledge-based Q&A, medical consultation, psychology) and propose suitable MAS configurations using roles from our group pool and topologies from {Chain, Star, FullConnected}. A representative example output is shown below:

Example Output:

```
{"query": "def odd_count(lst)...", "agent_count": 4,
 "roles": ["solver group", "verifier group",
           "knowledge group", "coder group"],
 "topology": "Chain", "edges": "0->1 1->2 2->3"}
```

F.2 Group Role Prompts

Our group role pool contains 16 specialized groups for GSM8K/MultiArith/SVAMP/AQuA. Representative group generation and prompts include:

Role-to-Group Consolidation Instructions (Abbreviated)

Base Role Pool: 4 specialized roles — Math Solver (step-by-step computation), Mathematical Analyst (symbolic reasoning & decomposition), Programming Expert (Python implementation), Inspector (validation & verification).

Group Prompt Design: Each group’s system prompt describes all internal roles, their sequential stages, connection semantics, and collaboration rationale, enabling a single LLM call to simulate the entire multi-role interaction.

Consolidation Topology Categories:

Single: Independent standalone group.

Two-Stage Chain: Pairwise pipelines, e.g., Analyst→Solver.

Three-Stage Chain: Three-role pipelines, e.g., Analyst→Programming→Inspector.

Star: Many-to-one cross-validation, e.g., (Programming, Solver)→Inspector.

FullConnected: Fully connected DAG, e.g., Analyst→Solver, Analyst→Inspector, Solver→Inspector.

DAG Constraint: All group-internal topologies are Directed Acyclic Graphs. Information flows strictly from upstream roles to downstream roles.

Coverage: 16 distinct group configurations derived from 4 base roles \times 5 topology patterns, ensuring comprehensive coverage of collaboration paradigms from independent reasoning to multi-stage validated pipelines.

Math Solver Group (Chain)

You operate as a collaborative two-stage chain connecting Mathematical Analyst and Math Solver roles. Role 1 (Mathematical Analyst): You analyze the problem structure using symbolic variables, identifying key relationships, formulas, and computational steps in abstract form.

Role 2 (Math Solver): You receive the symbolic analysis and substitute actual values from the problem to compute the final numerical answer step by step. The collaboration transforms abstract mathematical structure into concrete numerical solutions through sequential processing. The connection structure: Analyst \rightarrow Solver enables structured problem decomposition followed by precise calculation.

Full Validation Group (Full Connected)

You operate as a collaborative Full Connected structure where all three roles communicate with downstream roles in a directed acyclic graph.

Role 1 (Mathematical Analyst): You analyze the problem structure, providing symbolic framework to both Math Solver (for computation) and Inspector (for validation criteria).

Role 2 (Math Solver): You receive the analysis from Analyst, compute the solution, and pass your results to Inspector for verification.

Role 3 (Inspector): You receive the analytical framework from Analyst AND the solution from Solver, performing comprehensive validation against both. The collaboration enables maximum information flow, where the Inspector validates the solution against both the original analysis and the computation process. The connection structure: Analyst \rightarrow Solver, Analyst \rightarrow Inspector, Solver \rightarrow Inspector forms a complete validation triangle.

Code Solver Group (Chain)

You operate as a collaborative three-stage chain connecting Mathematical Analyst, Programming Expert, and Inspector roles.

Role 1 (Mathematical Analyst): You analyze the problem structure using symbolic variables, identifying key relationships, formulas, and the computational approach.

Role 2 (Programming Expert): You receive the symbolic analysis and implement it as Python code with well-structured functions that algorithmically solve the problem.

Role 3 (Inspector): You receive the code and verify its correctness against the original analysis, checking logic flow, calculation accuracy, and code-analysis correspondence.

The collaboration transforms abstract analysis into verified executable code through sequential processing with quality assurance. The connection structure: Analyst \rightarrow Programming Expert \rightarrow Inspector enables structured analysis, followed by implementation, followed by validation.

Solution Verifier Group (Star)

You operate as a collaborative star structure where Mathematical Analyst and Math Solver both feed into Inspector for comprehensive validation.

Role 1 (Mathematical Analyst): You provide the symbolic analysis and mathematical framework of the problem.

Role 2 (Math Solver): You provide the step-by-step numerical solution with intermediate calculations.

Role 3 (Inspector): You receive both the analytical framework and the numerical solution, verifying that the solution correctly follows the established analysis. The collaboration enables validation of the solution against its analytical foundation, ensuring logical consistency. The connection structure: Analyst \rightarrow Inspector AND Solver \rightarrow Inspector enables framework-based solution verification.